NANO LETTERS

XXXX
Vol. xx, No. x
-

Hierarchical Agglomerates of Carbon Nanotubes as High-Pressure Cushions

Yi Liu,[†] Weizhong Qian,[*,†] Qiang Zhang,[†] Anyuan Cao,[‡] Zhifei Li,[†] Weiping Zhou,[†] Yang Ma,[†] and Fei Wei[†]

Beijing Key Laboratory of Green Chemical Reaction Engineering and Technology, Department of Chemical Engineering, Tsinghua University, Beijing 100084, China, Department of Mechanical Engineering, University of Hawaii at Manoa, Honolulu, Hawaii 96822

Received December 25, 2007; Revised Manuscript Received March 4, 2008

ABSTRACT

We report the cushioning behavior of highly agglomerated carbon nanotubes. The nanotube agglomerates can be repeatedly compacted to achieve large volume reduction (>50%) and expanded to nearly original volume without structural failure, like a robust porous cushion. At a higher pressure range (10−125 MPa), the energy absorbed per unit volume is 1 order of magnitude higher than conventional cushion materials such as foamy polystyrene. The structure of hierarchical agglomerates can be controlled for tailoring the cushioning properties and obtaining a lower cushioning coefficient (higher energy absorption) over a wide range of pressures (1−100 MPa). The mechanism was studied in terms of morphology evolution of the nanotube aggregates and pore size distribution during compression.

Cushions are used for making surfaces or corners less hard, alleviating shock, and isolating vibration. Conventional materials such as wools, fibers, and foamy polymers (e.g., polystyrene) have been employed for decades.[1] We have seen a rapid development of microelectromechanical systems (MEMS) and nanoelectromechanical systems (NEMS) during past decades.[2,3] The device miniaturization demands novel buffering and cushioning materials and components that can be integrated into these microscale to nanoscale structures. Carbon nanotubes (CNTs) have shown excellent mechanical strength and the capability of producing large deformation without structural failure[4–6] and are considered as potential materials for constructing miniaturized cushioning devices.

Recently there has been a great interest in the compression behavior of aligned CNTs and applications such as impact resistance and damping.[7–14] CNTs were observed to form buckles that can fold tightly to allow large strain (>80%) compression.[7] Even after millions of compression cycles (at a set moderate strain), the CNTs show negligible mechanical and electrical property degradation.[8] With polymer infiltration, the CNT composites were capable of mechanical damping due to promoted interfacial friction between CNTs and the polymer matrix.[9] Elastic deformation of CNTs under compression has been observed in both static and high strain-rate (impact) tests.[7,8,11] These results suggest a promising application of CNTs as energy absorption structures (e.g., cushions), although the compression testing was done at relatively small stress levels (<20 MPa).[7,8]

We have made agglomerated multiwalled nanotubes by catalytic pyrolysis of propylene in a fluidized-bed reactor.[15] Simultaneous growth of multiple CNTs around a single catalyst particle floating in the furnace resulted in the formation of primary aggregates with a diameter of about 1 μm. The primary aggregates further combine with each other to form secondary aggregates with a larger size ranging from 10 μm to 1 mm. The size of secondary aggregates was controlled by the reaction time and gas velocity, and a superagglomerate of 1 mm diameter consists of about 10^7-10^{10} primary aggregates.[15] Transmission electron microscopy (TEM) characterization revealed that the CNTs in the agglomerates have an outer diameter of 8−20 nm and an inner diameter of 5−10 nm (corresponding to a wall number of 10−50) (Supporting Information Figure S1). The purity of as-grown agglomerates is above 90% (determined by thermal gravimetric analysis), with an estimated density of 400−500 g/L.

We have chosen a microagglomerate sample (10 μm aggregates, denoted as CNT-1) and a superagglomerate sample (average diameter of aggregates = 1 mm, denoted as CNT-2) for the current study. Purification of the metal catalyst was not processed here in order to maintain the agglomerate structures. About 10 g of each sample were loaded to the cavity of a cylindrical die, and a punch was fixed at the top of the die. Hydrostatic pressure was applied through an oil jack to push the die upward relative the punch

* Corresponding author. E-mail: qianwz@mail.tsinghua.edu.cn.
† Beijing Key Laboratory of Green Chemical Reaction Engineering and Technology, Department of Chemical Engineering, Tsinghua University.
‡ Department of Mechanical Engineering, University of Hawaii at Manoa.

10.1021/nl0733785 CCC: $40.75
Published on Web 04/03/2008

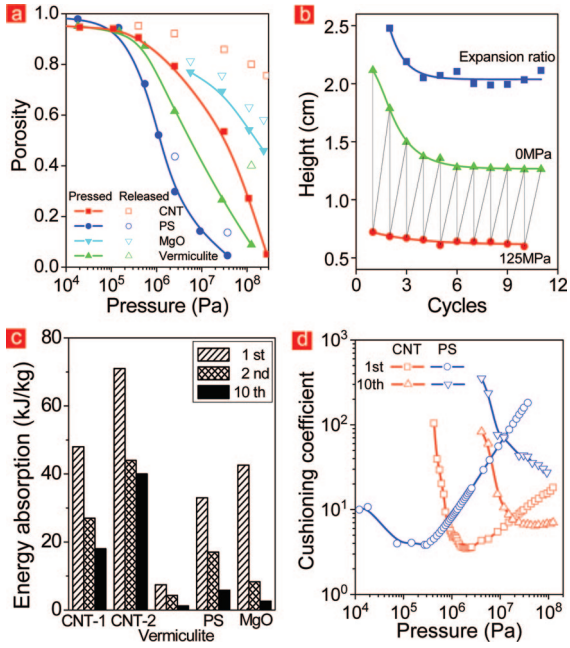

Figure 1. Cushioning properties of agglomerated CNTs. (a) Measurement of porosities of CNT-1 (microagglomerates), PS, vermiculite, and MgO nanoparticles at applied pressures from 10 kPa to 125 MPa and after pressure removal. (b) Compaction and shape (height) recovery of CNT-1. (c) Energy absorption during compression (at 125 MPa) of CNTs, vermiculite, PS, and MgO nanoparticles. (d) Cushioning coefficients of CNT-1 and PS at the 1st and 10th cycle, respectively.

so that CNT samples were compressed (Supporting Information Figure S2), during which the displacement and pressure were measured by micrometer caliper and pressure gauge for calculating the volume (or density) of the compacted sample, porosity (calculated by $\varepsilon = 1 - \rho/\rho_0$, where ρ is the green density of the compacted sampled and ρ_0 is the skeletal density of CNTs, which is assumed to be equal to that of graphite, e.g. 2.2 g/mL), and energy absorption density (area under the pressure−strain curve).

Compared with vertically aligned CNTs studied in literature,[7–14] there are a few distinct features of agglomerated random CNTs for cushioning applications. First, the growth of agglomerated CNTs is not confined by the substrate area, and large-scale production (on the order of kg) has been realized by the fluidized-bed reaction method developed in our laboratory.[15] Second, such agglomerates contain highly entangled CNTs with the potential of producing intense friction during deformation. Finally, the size of CNT agglomerates can be controlled from microscale to macroscale dimensions to tailor the cushioning properties, as discussed later.

The microagglomerates of CNTs (CNT-1) form a highly porous entanglement that can be compacted until a large volume reduction occurred (50−90%) by applying pressure and are able to recover to nearly original volume upon pressure release. Monitoring of the porosity of conventional packaging materials (e.g., PS, vermiculite) and nanoparticles (e.g., MgO) under different pressure values has revealed two features of CNT compaction (Figure 1a). First, the pores among CNT-1 can be completely removed at a pressure of ~250 MPa (corresponding to a porosity of zero). At the same pressure, MgO nanoparticles still maintain a porosity of about 50%. This result indicates that CNTs are flexible structures and could deform to close contact without any empty space left in the agglomerates. Second, after compression at a pressure of 100 MPa, CNT agglomerates can recover more than 80% porosity by expansion, indicating a highly resilient structure, whereas PS and vermiculite recovered less than 40% porosity at the same condition (Figure 1a). A good resilience was maintained in CNTs over a wide pressure range (10 kPa to 250 MPa), while PS and vermiculite degraded severely when the pressure reaches 10 MPa.

The recovery of porosity of CNT agglomerates can be directly observed from the height (volume) change of the samples filled in the die. Cyclic compression was performed with a preloading of 47 MPa, between a maximum and minimum pressure of 125 MPa and zero, respectively (Figure 1b). Initially, a densification (about 25% shrinkage of volume) was observed within the first five cycles, and after that the CNT agglomerates show a constant compaction and expansion ratio (≈2, defined as the free height over the height at full compression) for the following cycles (Figure 1b). In comparison, PS, vermiculite, and MgO show negligible expansion after being compressed by high pressure (Supporting Information Figure S3). Such a property of CNTs, being able to deform under pressure and then recover original shape, is strongly desired for cushioning materials.

The energy absorbed per unit mass during compression (125 MPa) of the materials included in Figure 1a has been calculated and summarized in Figure 1c. Both CNT samples (with μm or mm aggregates) show much enhanced energy absorption (six times higher at cycle 10) than PS, vermiculite, and MgO nanoparticles. A value of 70 kJ/kg from CNTs is also much higher than reported metallic (e.g., aluminum, iron) foams.[16] Although the absorption decreases after repeated compression, the tendency of saturation observed in Figure 1b promises the capability of energy absorption for many cycles with minimized degradation.

Static cushioning coefficient (C), defined as $C(\sigma_{max}) = \sigma_{max}/(\int_0^{\varepsilon} \sigma\, d\varepsilon)$,[17] where ε is strain and σ is stress, provides a measure of absorbed energy per unit volume for a set pressure (σ_{max}) compression. We have measured the cushioning coefficients of agglomerated CNTs and PS over a wide range of set pressures (10 kPa to 125 MPa) (Figure 1d). The coefficient of PS is small ($C < 10$) at a relatively lower pressure range (<1 MPa) but arises rapidly upon increasing pressure. In addition, the coefficient of PS remains a high value ($C > 30$) after repeated compression at pressures above 1 MPa (Figure 1d). On the contrary, CNTs show a lower cushioning coefficient (higher energy absorption) at relatively higher pressures. After 10 compression cycles, the value of coefficient has decreased to <10 over a pressure range of 10−125 MPa (Figure 1d). These results revealed a suitable pressure range for PS (<1 MPa) and CNTs (>10 MPa) to work as cushions, respectively.

We have investigated the effect of different CNT agglomerate structures on the cushioning behavior. Micrometer and millimeter agglomerates (CNT-1 and CNT-2), as shown

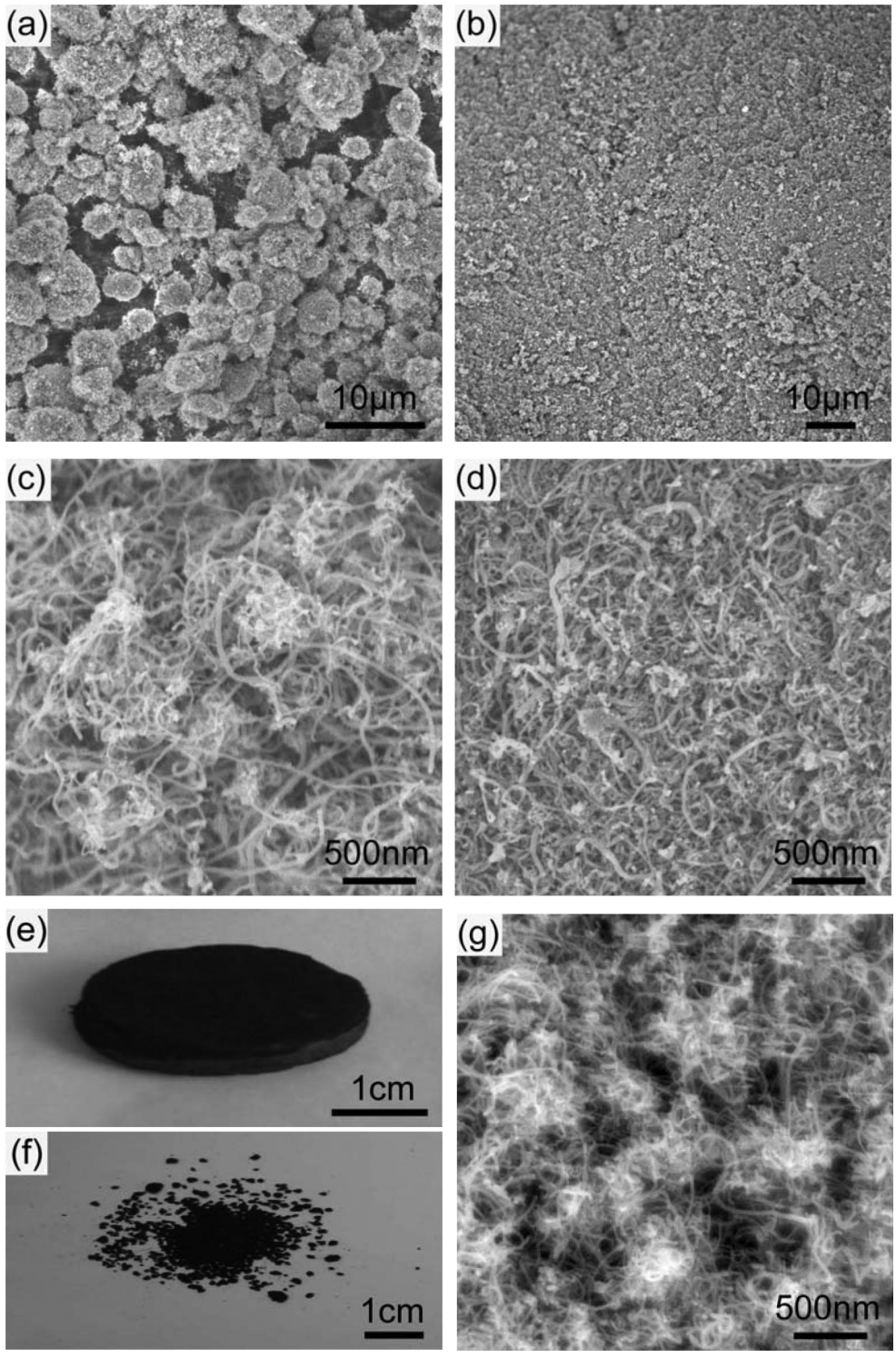

Figure 2. Characterization of agglomerated CNTs. (a) Microagglomerates of CNT-1 (average size $<10\ \mu$m). (b) Image of the surface area of a superagglomerate of CNT-2 (average agglomerate size is 1 mm). (c) Primary aggregates of CNT-1 observed at a pressure of 3 MPa. (d) Breakdown of CNT-1 at a pressure of 30 MPa, resulting in a relatively uniform structure (versus aggregates). (e) A block of CNTs formed after breakdown of agglomerates. (f) Superagglomerates without collapsing after compression. (g) SEM image of CNT-2 after compression, showing that the structure of primary aggregates has been retained.

in parts a and b of Figure 2, were studied. Pore size distribution shows that the agglomerates of CNT-2 have a more compacted structure than CNT-1, where pores smaller than 100 nm occupy a higher percentage, consistent with the sub-micrometer primary aggregates structure of CNT-2 (Supporting Information Figure S4). Characterization by scanning electron microscope (SEM) has revealed the morphology change, where micrometer-scale primary agglomerates of CNT-1 collapsed into a rather uniform entanglement at a compressive pressure of >30 MPa (Figure 2c,d). Once the CNTs agglomerates broke down and coalesced under pressure, they can not recover to original

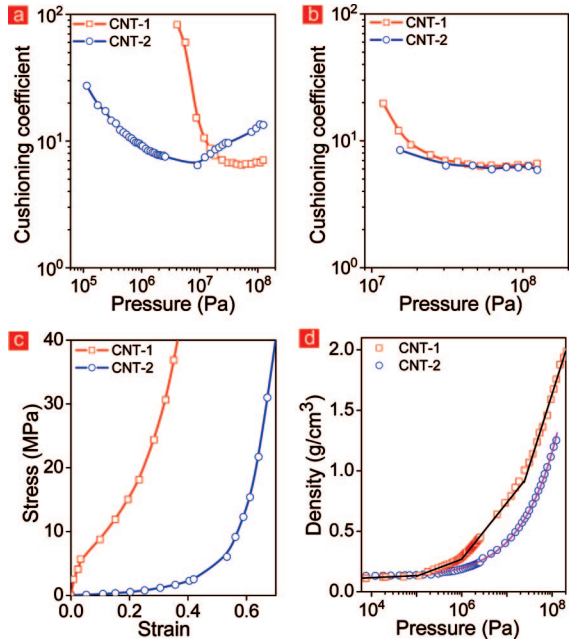

Figure 3. Tailoring cushioning properties. (a) Cushioning coefficients of microagglomerates (CNT-1) and superagglomerates (CNT-2) for 10th cycle. (b) Coefficients of CNT-1 and CNT-2 with precompression at 10 MPa. (c) Strain−stress curves of CNT-1 and CNT-2 for the 10th cycle. (d) Density change of CNT agglomerates during compaction.

structure after removal of pressure. The process of local structure change of CNT-1 under compression was shown in Supporting Information Figure S5. The CNTs formed an integral piece of block after taken out of the cylindrical die (Figure 2e). In contrast, superagglomerates (about 1 mm in diameter) of CNT-2 did not collapse at high pressure (e.g., 100 MPa) and maintained original structure after removal from the die (Figure 2f). SEM image of CNT-2 after compression shows that the structure of primary aggregates has been retained (Figure 2g). The coalesced agglomerates as shown in Figure 2d were more condensed compared with secondary agglomerates in Figure 2g, and their bulk densities and porosity could be considerably different based on SEM characterizations. Several factors may be involved in the unique cushioning behavior, including agglomerate size, pore size, and local structures. The primary aggregates have smallest size, and the hard catalyst core might have pronounced effect on mechanical properties. When they further combined into larger agglomerates (via Van der Waals force), the sponge behavior could be enhanced due to increased porosity.

The superagglomerates (CNT-2) show a much smaller cushioning coefficient than the microagglomerates (CNT-1) at a relatively lower pressure range (<10 MPa) for the 10th cycle (Figure 3a). This is because the superagglomerates are capable of protecting the original structure from being completely collapsed (Figure 2f,g) and maintaining a higher-level porosity after repeated compression potentially useful for energy absorption. The stress−strain curves (for 10th cycle) show that at a pressure of 10 MPa, the compressive strain of CNT-1 is only 15% while the strain of CNT-2 reaches nearly 60% (due to higher porosity) (Figure 3c). At pressures above 10 MPa, compression and/or collapsing of primary aggregates were taken into account and therefore CNT-2 shows higher cushioning coefficient. Nonetheless, we found that a precompression at 10 MPa to reduce larger pores in loose structures resulted in significant decrease of cushioning coefficient (from >10 to a value of about 6) of superagglomerated CNTs that is approaching CNT-1 (Figure 3b). Therefore, the cushioning coefficient of CNTs could be improved (to be lower than 10) over a wide range of maximum compressive pressure (1−100 MPa) by tailoring the agglomerate structure, while PS materials only work at a much smaller pressure range (<1 MPa). Preliminary tests on vertically aligned CNT films,[18] which were removed from the substrate and stacked in the die cavity randomly, have shown a coefficient value in between agglomerated CNTs (CNT-1 and CNT-2) (Supporting Information Figure S6).

The pore size evolution during compression was monitored by the Hg penetration method.[19] The microagglomerates (CNT-1), initially having a pore size range of 40 nm to μm, have converged into a narrow distribution around 10 nm due to high pressure compression (100 MPa) (Supporting Information Figure S7), which is consistent with the observation of the breakdown of agglomerates (Figure 2c,d). However, the superagglomerates (CNT-2) maintain a pore size distribution of 0.3−6 μm constantly when compressed to high pressure (Supporting Information Figure S7), implying that the agglomerates did not collapse completely as can be seen in Figure 2g. Stress−strain curves also revealed that: (1) for CNT-1, microscale pores (associated with primary aggregates) were compressed at the beginning stage (ε < 20%) accompanied with a higher slope (modulus) of the curve, and (2) for CNT-2, large pores (associated with millimeter-scale aggregates) were compressed first with a much smaller modulus (Figure 3c).

During compression, the increase of density of CNT-1 shows three turning points at about 0.1, 1, and 30 MPa (Figure 3d). The lack of abrupt points in the density−pressure curve of CNT-2 suggests the interactions between agglomerates in CNT-1. Niesz et al. have related the turning points to the breakdown of submicrometer alumina aggregates.[20] Our CNT products actually consist of a hierarchical assembly of agglomerates built from primary aggregates (about 1 μm in diameter) until the macroscopic level (tens of micrometers for CNT-1 and 1 mm for CNT-2), and the breakdown might occur from the highest level (aggregates of tens of micrometers) downward, resulting in multiple events (turning points) for CNT-1 under pressure.

In conclusion, CNTs have shown a good cushioning performance at a relatively higher pressure range (1−100 MPa), while conventional materials (e.g., PS, vermiculite) mainly work at much smaller pressure. The deformation of entangled CNTs and breakdown of agglomerates are possible factors accounting for energy absorption. The cushioning properties of CNTs could be further improved by tailoring the size of agglomerates and manipulating the interactions between agglomerates. Future experiments include fabrication of highly pure, metal-free CNT cushions after removal

of the catalyst core in agglomerates such as by high temperature evaporation.

Acknowledgment. This work was supported by NSFC key program (no. 20236020), NSFC (no. 20606020), FANEDD (no. 200548), Chinese national program (2006CB932702), Key Project of Chinese Ministry of Education (no. 106011).

Supporting Information Available: TEM characterization of primary CNT agglomerates. Scheme of the equipment for compression tests. Expansion ratios of CNTs, MgO nanoparticles, vermiculite and PS. Pore size distribution of CNT-1 and CNT-2. SEM morphologies of agglomerates in CNT-1 after compacting under different pressures. Cushioning coefficients of agglomerated and vertically aligned CNTs. Ex-situ pore size distribution of CNTs after being compressed at different pressures. This material is available free of charge via the Internet at http://pubs.acs.org.

References

(1) http://en.wikipedia.org/wiki/Cushioning.
(2) Craighead, H. G. *Science* **2000**, *290*, 1532–1535.
(3) Peterson, K. E. *IEEE Trans. Electron Devices* **1978**, *25*, 1241.
(4) Falvo, M. R.; Clary, G. J.; Taylor, R. M., II; Chi, V.; Brooks, F. P., Jr.; Washburn, S.; Superfine, R. *Nature* **1997**, *389*, 582–584.
(5) Qian, D.; Wagner, G. J.; Liu, W. K.; Yu, M. F.; Ruoff, R. S. *Appl. Mech. Rev.* **2002**, *55*, 495–533.
(6) Tang, J.; Qin, L.-C.; Sasaki, T.; Yudasaka, M.; Matsushita, A.; Iijima, S. *Phys. Rev. Lett.* **2000**, *85*, 1887–1889.
(7) Cao, A. Y.; Dickrell, P. L.; Sawyer, W. G.; Ghasemi-Nejhad, M. N.; Ajayan, P. M. *Science* **2005**, *310*, 1307–1310.
(8) Suhr, J.; Victor, P.; Ci, L.; Sreekala, S.; Zhang, X.; Nalamasu, O.; Ajayan, P. M. *Nature Nanotechnol.* **2007**, *2*, 417–421.
(9) Suhr, J.; Koratkar, N.; Keblinski, P.; Ajayan, P. *Nat. Mater.* **2005**, *4*, 134–137.
(10) Daraio, C.; Nesterenko, V. F.; Jin, S. *Appl. Phys. Lett.* **2004**, *85*, 5724–5726.
(11) Daraio, C.; Nesterenko, V. F.; Jin, S.; Wang, W.; Rao, A. M. *J. Appl. Phys.* **2006**, *100*, 064309.
(12) Teo, E. H. T.; Yung, W. K. P.; Chua, D. H. C.; Tay, B. K. *Adv Mater.* **2007**, *19*, 2941–2945.
(13) Deck, C. P.; Flowers, J.; Mckee, G. S. B.; Vecchio, K. *J. Appl. Phys.* **2007**, *101*, 023512.
(14) Pushparaj, V. L.; Ci, L. J.; Sreekala, S.; Kumar, A.; Kesapragada, S.; Gall, D.; Nalamasu, O.; Ajayan, P. M. *Appl. Phys. Lett.* **2007**, *91*, 153116.
(15) Hao, Y.; Zhang, Q. F.; Wei, F.; Qian, W. Z.; Luo, G. H. *Carbon* **2003**, *41*, 2855–2863.
(16) Park, C.; Nutt, S. R. *Mater. Sci. Eng. A* **2000**, *288*, 111–118.
(17) Avalle, M.; Belingardi, G.; Montanini, R. *Int. J. Impact. Eng.* **2001**, *25*, 455–472.
(18) Zhang, Q.; Zhou, W. P.; Qian, W. Z.; Xiang, R.; Huang, J. Q.; Wang, D. Z.; Wei, F. *J. Phys. Chem. C* **2007**, *111*, 14638–14643.
(19) Palacio, L.; Prádanos, P.; Calvo, J. I.; Hernández, A. *Thin Solid Films* **1999**, *348*, 22–29.
(20) Niesz, D. E.; Bennett, R. B.; Snyder, M. J. *Am. Ceram. Soc. Bull.* **1972**, *51*, 677–680.

NL0733785